Molecular Crystals and Liquid Crystals

ISSN: 1542-1406 (Print) 1563-5287 (Online) Journal homepage: http://www.tandfonline.com/loi/gmcl20

Electrochemical characterizations and the effect of glycerol in biopolymer electrolytes based on methylcellulose-potato starch blend

Y. M. Yusof & M. F. Z. Kadir

To cite this article: Y. M. Yusof & M. F. Z. Kadir (2016) Electrochemical characterizations and the effect of glycerol in biopolymer electrolytes based on methylcellulose-potato starch blend, Molecular Crystals and Liquid Crystals, 627:1, 220-233, DOI: 10.1080/15421406.2015.1137115

To link to this article: http://dx.doi.org/10.1080/15421406.2015.1137115

Published online: 13 May 2016.

MOL. CRYST. LIQ. CRYST.
2016, VOL. 627, 220–233
http://dx.doi.org/10.1080/15421406.2015.1137115

Taylor & Francis
Taylor & Francis Group

Electrochemical characterizations and the effect of glycerol in biopolymer electrolytes based on methylcellulose-potato starch blend

Y. M. Yusof[a] and M. F. Z. Kadir[b]

[a]Institute of Graduate Studies, University of Malaya, Kuala Lumpur, Malaysia; [b]Centre for Foundation Studies in Science, University of Malaya, Kuala Lumpur, Malaysia

ABSTRACT

Polymer electrolytes have been prepared by blending methylcellulose (MC)-potato starch, doped with lithium perchlorate ($LiClO_4$) and plasticized with glycerol. The blend of 60 wt% MC-40 wt% starch was found to be the most suitable ratio to serve as polymer host. Fourier transform infrared (FTIR) spectroscopy analysis proved the interaction among the components. X-ray diffraction (XRD) analysis indicated that the conductivity enhancement is due to the increase in amorphous content. The highest ionic conductivity obtained at room temperature was $(4.25 \pm 0.82) \times 10^{-4}$ S cm^{-1} for MC-starch-$LiClO_4$-20 wt% glycerol. The highest conducting samples in both systems were found to obey Arrhenius rule. Dielectric study further strengthens the conductivity result.

KEYWORDS

Polymer electrolyte; conductivity; methylcellulose-starch blend; lithium perchlorate; XRD

Introduction

Solid polymer electrolyte (SPE) has a good potential in lithium batteries, fuel cells, sensors and electrochemical devices [1–4]. Researchers reported that this type of electrolyte produced reasonable potential window stability, easy to prepare and have a good thermal stability [5–7]. Various efforts have been done to enhance the ionic conductivity of SPE including plasticization [8, 9], polymer blending [10, 11], addition of ceramic filler [12, 13] and copolymerization [14]. This is because electrolyte is the key component of electrochemical devices since it provides the medium for ionic conduction [15].

Blending polymers is an effective way for achieving suitable combinations of physical properties and better characteristics. The most important factor to choose the polymer blends is the miscibility of the components [16]. Cellulose derivatives are polysaccharides composed of linear chains of $\beta(1–4)$ glucosidic units with methyl, hydroxypropyl or carboxyl substituents [17]. Methylcellulose (MC) has an excellent film-forming property, water solubility, and efficient oxygen permeabilities [18]. Starch has attracted researchers for its rich variety and abundance in nature. It is composed of repeating 1,4-α-D-glucopyranosyl units: amylose and amylopectin [19–21]. Starch is soluble in water, however the molded articles prepared from starch and water was transparent, brittle and sensitive to atmospheric moisture [22]. Therefore, blending two or more dissimilar natural polymers has shown potential to overcome these difficulties. Khiar and Arof [23] reported that the ionic conductivity of 2.83×10^{-5} S cm^{-1} at

CONTACT M. F. Z. Kadir mfzkadir@um.edu.my
Color versions of one or more of the figures in the article can be found online at www.tandfonline.com/gmcl.

room temperature obtained from starch doped with NH_4NO_3 has increased to 3.89×10^{-5} S cm^{-1} by blending starch and chitosan [24].

Ions are mainly mobile in amorphous phase since their motion is supported by polymer segmental motion [25, 26]. The percentage of amorphous nature of the polymer can be increased by the addition of salts [27]. In this work, $LiClO_4$ has been chosen as the dopant due to its low lattice energy. $LiClO_4$ is comprised of small sized cation and large sized anion which is believed can give high conductivity to the electrolytes due to its high diffusion rate of ions [28].

Experimental

Electrolytes preparation

Different weight percentages (x wt%) of potato starch (Sigma Aldrich) were dissolved in 100 mL of 1% acetic acid (SYSTERM) and heated at 80°C for 20 min. After the solutions cooled to room temperature, (100−x) wt% of MC was then added to the solutions. The mixtures were stirred until homogeneous solutions obtained. For preparation of salted system, different amounts of $LiClO_4$ (Sigma Aldrich) were added to the starch-MC solutions and stirred until they become homogeneous solutions. For preparation of plasticized system, different amounts of glycerol (SYSTERM) were added into the highest conducting electrolyte in the salted system and stirred until complete dissolution. All solutions were cast into different plastic Petri dishes and left to dry for 2–3 days at room temperature. The dried films were then kept in a desiccator filled with silica gel desiccants for further drying to avoid any trace moisture.

Electrolytes characterization

XRD measurements of the electrolytes were conducted using Siemens D5000 X-ray diffractometer, where X-rays of 1.5406 Å wavelengths were generated by a Cu Kα source. The 2θ angle was varied from 5° to 80°. Thermogravimetric analysis (TGA) was carried out using Perkin-Elmer Pyris 1 TGA equipment. The samples were heated from room temperature to 700°C at a heating rate of 10°C min^{-1}. The FTIR studies were performed using Spotlight 400 Perkin-Elmer spectrometer in the wavenumber range of 400 – 4000 cm^{-1} at a resolution of 1 cm^{-1}. Confirmation of interaction between polymer and salt was the objective of performing FTIR studies. Impedance measurements were carried out using HIOKI 3532–50 LCR HiTESTER in the frequency range of 50 Hz to 5 MHz. The electrolytes were sandwiched between two stainless steel electrodes of a conductivity holder. The conductivity of the electrolyte was calculated using:

$$\sigma = \frac{t}{R_b A} \tag{1}$$

where t is the thickness of the electrolyte, R_b is the bulk resistance and A is the electrode electrolyte contact area.

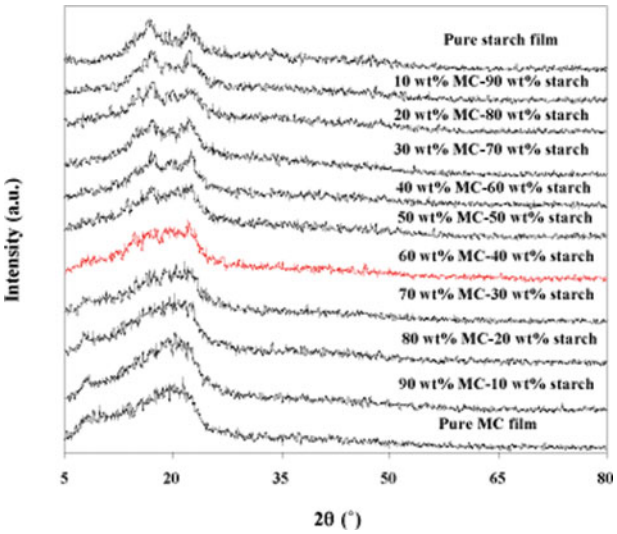

Figure 1. X-ray diffraction patterns of MC-starch polymer blend.

Results and discussion

Characteristics of polymer blend films

The XRD patterns of MC-starch polymer blends are represented in Fig. 1. The choice of the most suitable ratio of the polymers to serve as polymer host is directed to the reduced in crystallinity. From the X-ray diffractogram, it can be seen that MC film exhibits a peak at 2θ=8° and a broad peak at 21°, while starch film exhibits an unresolved doublet at 2θ= 19 and 20°, and also another two peaks at 2θ= 17 and 22°, which almost similar with the one reported by El-Kader & Ragab [29]. The presence of the peak at 2θ=8° in the XRD pattern of MC film is correlated with the crystallinity of trimethyl glucose sequence [30]. However, in the blend of 60 wt% MC and 40 wt% starch, all crystalline peaks have disappeared inferring that the blend is well formed and miscible into each other. The crystallinity of each polymer is strongly affected by the presence of the other component. Hence, molecular miscibility between the components of the polymer blends could favor the formation of a good polymer host. To strengthen the XRD results, crystallinity values have been calculated using equation:

$$\chi_c = \frac{c}{c+a} \times 100\% \tag{2}$$

with the aid of Origin 9.0 software, where c is the crystalline area and a is the amorphous area of the electrolyte [31]. The crystallinity values are listed in Table 1. The blend of 60 wt% MC and 40 wt% starch gives the lowest degree of crystallinity value compared to other blends.

TGA measurement has been carried out to study the thermal analysis and phase transition of the polymer blend films. As the temperature increased up to 100°C, an initial thermal degradation around 10% is detected due to evaporation of moisture. The elimination of impurities in the polymer electrolytes and residual solvent also contributes to the weight loss at this stage [32]. Figure 2 shows that starch starts to decompose around 250°C, while MC starts to decompose around 340°C which means that MC can stand higher temperature compared to starch. Other researchers also reported almost similar TGA results for cellulose derivatives degradation process, which occurred due to the formation of levoglucosan and other volatile compounds [33, 34]. According to Ramesh et al. [35], this one step weight loss process of

Table 1. Degree of crystallinity of polymer blend films.

Samples	Degree of crystallinity
Pure starch film	37.76
10 wt% MC-90 wt% starch	34.22
20 wt% MC-80 wt% starch	32.66
30 wt% MC-70 wt% starch	32.49
40 wt% MC-60 wt% starch	30.68
50 wt% MC-50 wt% starch	29.76
60 wt% MC-40 wt% starch	28.80
70 wt% MC-30 wt% starch	32.07
80 wt% MC-20 wt% starch	35.86
90 wt% MC-10 wt% starch	36.57
Pure MC film	39.35

starch is attributed to the depolymerization of the polymer electrolyte. During this process, the monomers, which are amylose and amylopectin detached from their long polymer chain while forming aromatic and cross-linked structures as the temperature increases [36].

Starch and MC have different molecular structures even though both are natural polymers. Starch consists of highly branched amylopectin and linear amylose, which exist in the form of granules [37]. The highly branched of amylopectin are difficult to be disrupted, hence left around 20% residues at 700˚C. Mano et al. [36] also mentioned in their report that the residues left at 500˚C was about 20% due to the different degradation rate of amylose and amylopectin. While in MC, COO^- group exists which is decarboxylated and enhanced the rapid loss in the temperature range between 200˚C to 400˚C [32]. The final stage of the MC film in the present work represents that all the residuals have evaporated. Guru et al. [38] exhibited a 100% weight loss of MC around 380˚C compared to PVA that only decomposed around 80% at 400˚C.

When two polymers are mixed or blended together, thermal behaviors from both polymers are retained in the blended film. For instance, Jingjid et al. [39] reported that the final residue of MC at 440˚C was around 14%. However, the decomposition temperature of the blend of

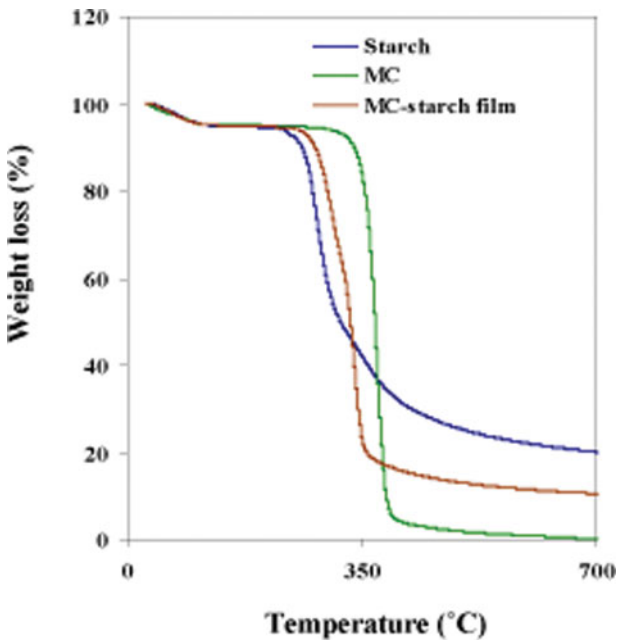

Figure 2. TGA results of MC powder, starch powder and MC-starch blend film.

montmorillonite with MC has increased as the final residue also increased up to 24%. This indicates that the MC and montmorillonite are compatible and the thermal stability has been improved if compared to MC. In the present work, it is observed that blending MC and potato starch has improved the thermal stability since the blend film starts to decompose at around 280˚C. At 700˚C, the degradation behavior of potato starch and MC are retained in the MC-starch blend film where it shows around 10% materials left. Hence, based on these XRD and TGA results, the polymer blend consists of 60 wt% MC and 40 wt% starch is expected to host a reasonable fast ionic conduction due to its amorphous nature and improved thermal stability compared to other blend compositions.

FTIR study

Figure 3 exhibits the FTIR spectra of MC powder, MC film and MC-starch blend film. The ether band is observed at 1046 and 1101 cm^{-1} for the MC powder. In the MC film, a slight change has occurred to the peak due to the complexation of the C-O-C stretching group with the solvent. This result is almost similar with the region reported by Aziz et al. [40], which further shifted during the complexation of MC and starch in the MC-starch blend film. The addition of $LiClO_4$ leads to the shifting of the ether peak towards lower wavenumber as can be seen in Figure 4(a) which is the same phenomena as reported by Kulasekarapandian et al. [41]. The band observed at around $\sim$ 1100 cm^{-1} starts to disappear as $LiClO_4$ content increased. This indicates the interaction between Li^+ cation and oxygen atom in C-O bond of MC, which acts as electron donor [11]. The addition of $LiClO_4$ has increased the amorphousness of the polymer electrolyte, which support the motion of the charge carriers hence increased the conductivity. Figure 4(b) depicts FTIR spectra of MC-starch-$LiClO_4$-glycerol in the ether region. It can be seen that the C-O-C band has shifted towards lower wavenumbers due to the interaction among the components of the polymer blend. This proves that the glycerol has played the role as transit site for ion conduction in the plasticized system.

Conductivity study

Figure 5(a) represents the variation of room temperature conductivity as a function of $LiClO_4$ concentration. Conductivity of electrolytes depends on charge carrier concentration [42]. It can be seen that the conductivity increased to $(3.26 \pm 1.12) \times 10^{-6}$ S cm^{-1} as the $LiClO_4$ concentration increased up to 20 wt%. This conductivity can be compared with the work done by Sudhakar et al. [43]. They reported a conductivity value of $\sim 10^{-6}$ S cm^{-1} obtained from the unplasticized chitosan-poly (ethylene glycol)(PEG)-$LiClO_4$. Further addition of salt has lead to the conductivity decrement because the distance between the dissociated ions become closer causes the ions to reassociate back to become neutral ion pairs which do not contribute in ion conduction [4]. The variation of room temperature conductivity as a function of glycerol content is shown in Fig. 5(b). Different amounts of glycerol (5–30 wt%) were added to the highest conducting electrolyte in the salted system in order to enhance the conductivity. The conductivity value has increased to $(4.25 \pm 0.82) \times 10^{-4}$ S cm^{-1} on the addition of 20 wt% glycerol. A plasticizer has a high dielectric constant that can weaken the Columbic force between the anion and cation of the salt thus easier for the salt to dissociate to become free mobile ions [4, 44]. Besides, the addition of glycerol can create more favorable pathways for lithium ions conduction hence increase the ionic mobility [45, 46]. However, further addition of glycerol leads to conductivity decrement due to the formation of microcrystalline junctions between the plasticizer which causes the recrystallization of salt [47, 48]. The host

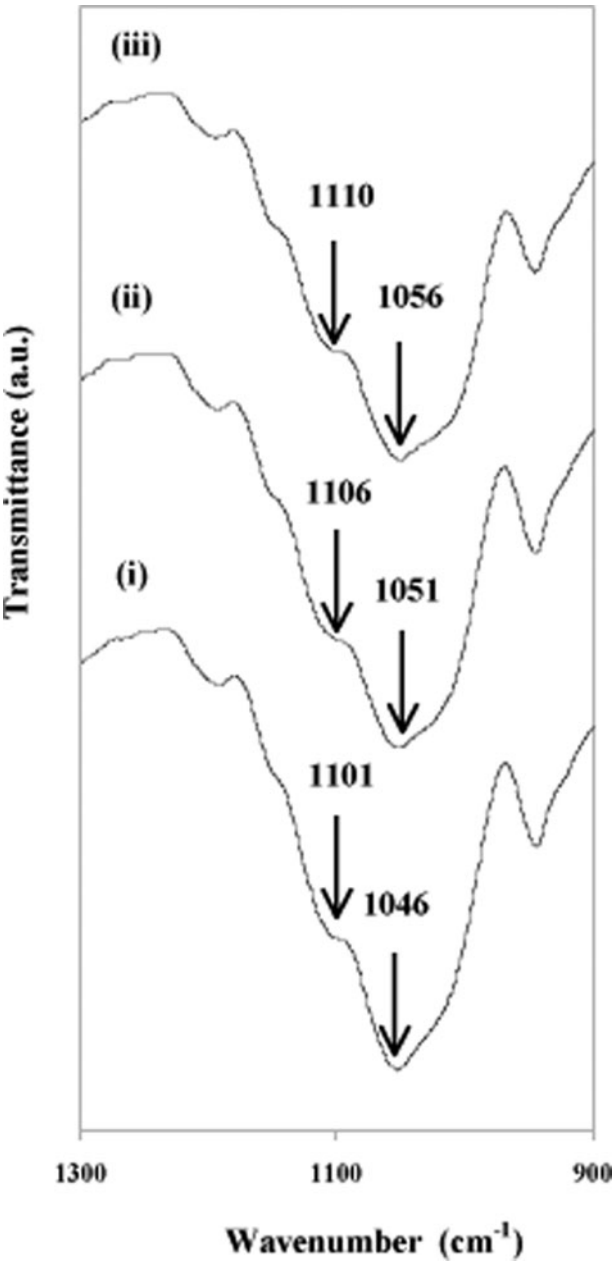

Figure 3. (a) FTIR spectra for (i) MC powder, (ii) pure MC film and (iii) 60 wt% MC-40 wt% starch blend film in the region of 900–1300 cm^{-1}.

polymer has also been displaced by the plasticizer molecules within the salt complexes [49]. Pawlicka et al. [50] reported a conductivity value of 6.12×10^{-5} S cm^{-1} for the starch-$LiClO_4$-glycerol system at room temperature which is lower compared to this work. Buraidah and Arof [51] reported that more complexation sites can be provided by blending two polymers. This method provides more sites for ion migration and exchange to take place which leads to an increase in conductivity. It was proven by their work when the conductivity of 55 wt% chitosan-45 wt% NH_4I had been increased from 3.73×10^{-7} S cm^{-1} to 1.77×10^{-6} S cm^{-1} when chitosan was blended with poly(vinyl alcohol) (PVA). Kulasekarapandian et al. [41] also

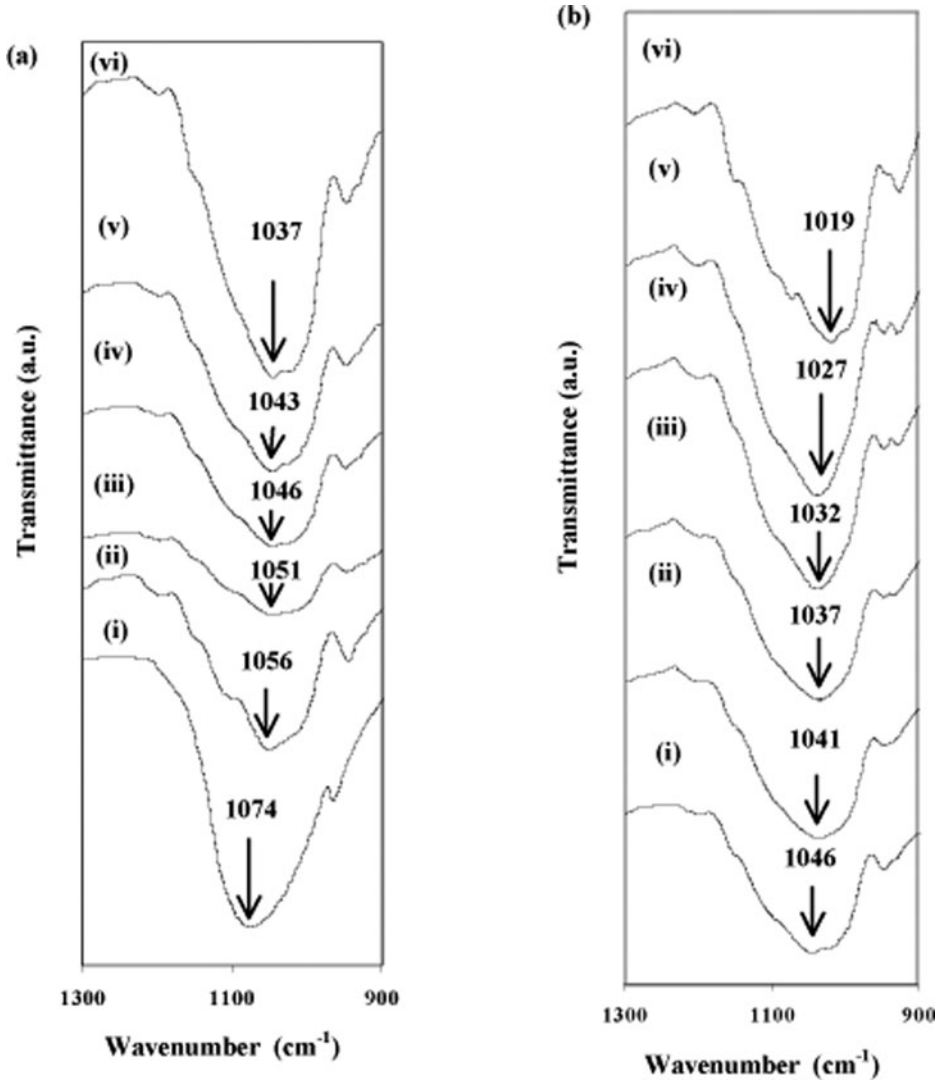

Figure 4. (a) FTIR spectra for (i) pure $LiClO_4$ (ii) pure MC-starch film (iii) MC-starch-10 wt% $LiClO_4$ (iv) MC-starch-20 wt% $LiClO_4$, (v) MC-starch-30 wt% $LiClO_4$ and (vi) MC-starch-40 wt% $LiClO_4$ in the region of 900–1300 cm^{-1}. (b) FTIR spectra for (i) MC-starch-20 wt% $LiClO_4$ film with (ii) 5 wt% glycerol, (iii) 10 wt% glycerol, (iv) 15 wt% glycerol, (v) 20 wt% glycerol and (v) 25 wt% glycerol in the region of 900–1300 cm^{-1}.

reported that the blend of 37.5% PVC-37.5% PEO-25% $LiClO_4$ exhibits a conductivity value of 6.50×10^{-6} S cm^{-1}.

The plots of conductivity as a function of temperature for the highest conducting sample in salted and plasticized systems are shown in Fig. 6. Since the regression values, R^2 are nearly to 1, it can be implied that the plots of log σ versus $1000/T$ are Arrhenian [52], which follow the equation:

$$\sigma = \sigma_0 \exp\left[\frac{-E_a}{kT}\right] \tag{3}$$

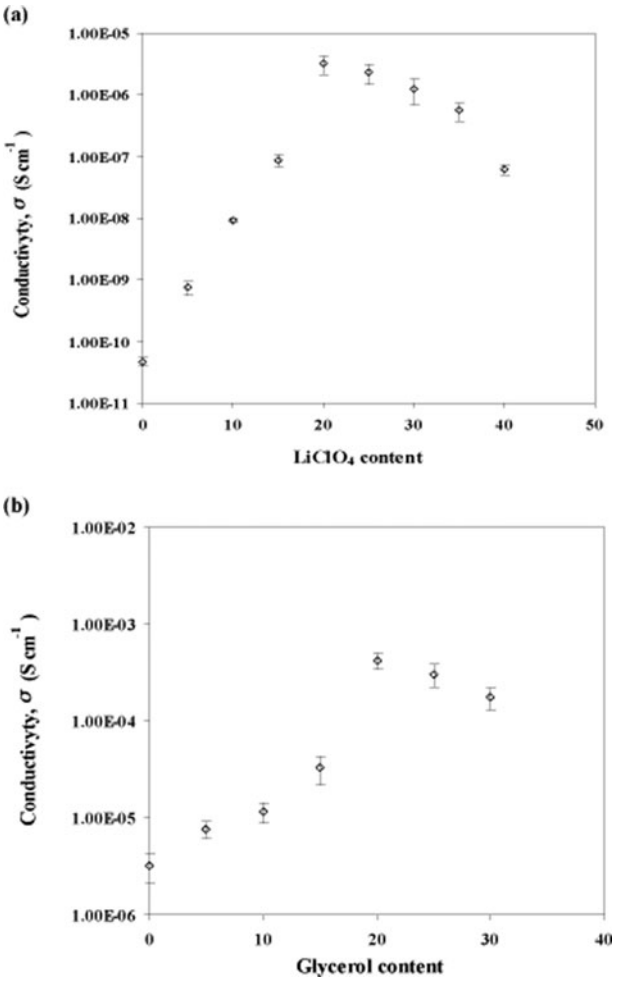

Figure 5. Effect of (a) $LiClO_4$ concentration and (b) glycerol concentration on conductivity at room temperature.

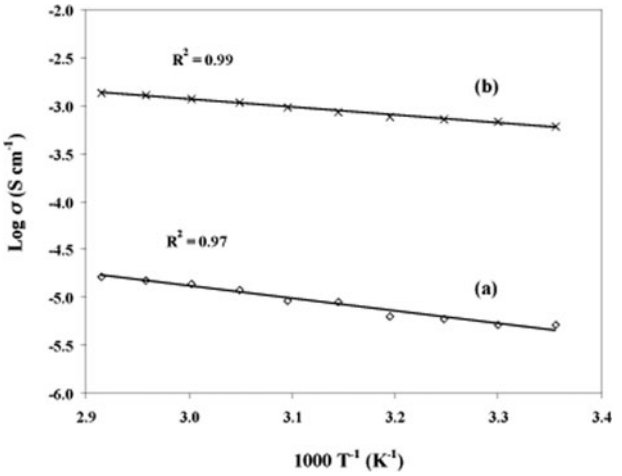

Figure 6. Effect of temperature on conductivity for (a) MC-starch-20 wt% $LiClO_4$ and (b) MC-starch-$LiClO_4$-20 wt% glycerol electrolytes.

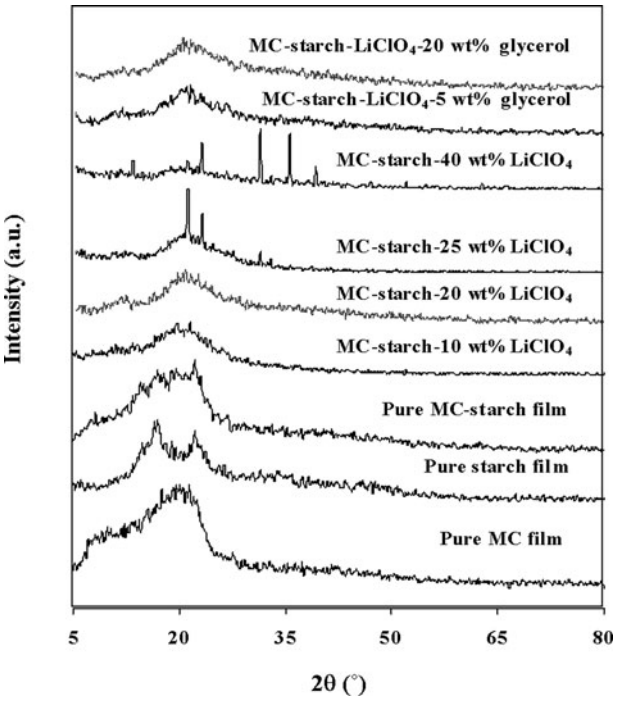

Figure 7. X-ray diffraction patterns of selected samples.

where σ_0 is a pre-exponential factor, E_a is the activation energy of conduction and k is Boltzmann constant. From the plot, it is depicted that the conductivity increased as the temperature increased which attributed to the increase in number density and mobility of ions [53]. Besides, at high temperature, the polymer chain acquires faster internal modes where bonding rotations produce motions to favor inter and intra-chain ion hopping [54]. Using the slope of the Arrhenius plots, the E_a values for the highest conducting sample in salted and plasticized systems are found to be 0.258 and 0.165, respectively. These results imply that the ions in highly conducting samples require lower energy for migration [51]. Lower E_a is resulted from the short distance between the transit sites provided by the blended polymers [51]. Based on Anderson-Stuart model [55], E_a is the sum of the binding energy of the ion to its site and the kinetic energy for migration. If the energy of the ion is only sufficient to overcome the binding energy, the ion will not migrate but instead, dislocated from its site but will still remain at the same location. If it has more energy than the binding energy, the ion will be free to move [45].

XRD study

The X-ray diffractograms of selected samples in salted and plasticized systems is depicted in Fig. 7. Hodge et al. [56] suggested that XRD patterns with no obvious peak proved that the salt is completely dissociated in a polymer matrix. It can be seen that the addition of 10 wt% $LiClO_4$ has increased the amorphousness of the polymer blend by reducing the intensity of the crystalline peaks at $2\theta = 20$ and 22° compared to pure MC-starch film. The highest room temperature conductivity for the salted system has been attained with the addition of 20 wt% $LiClO_4$ which proved by further suppressed of the crystalline peaks. This indicates that the presence of $LiClO_4$ contributes a lot to the amorphousness of the polymer blend by increasing the number of mobile charge carriers [57]. However, the addition of more than 20 wt% of

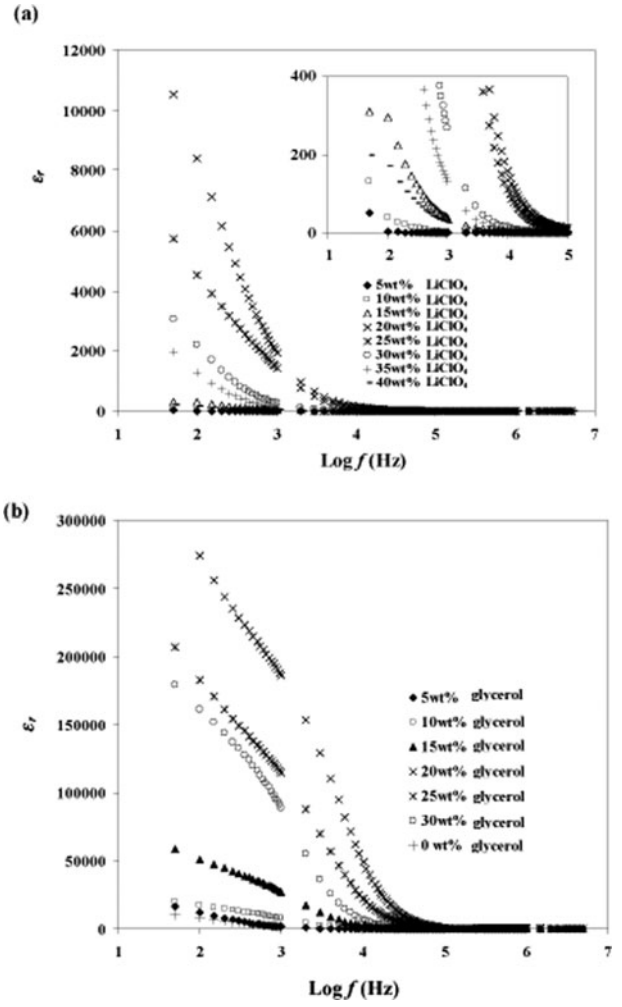

Figure 8. Plots of ε_r versus frequency for (a) salted and (b) plasticized systems. The inset figure in (a) shows an enlarge plot at low frequency.

$LiClO_4$ leads to an increase in crystallinity. It can be seen from the diffractograms that the crystalline peaks due to excess of salt start to appear at 2θ=21, 23, 31, 35 and 39° which is similar as reported by Kulasekarapandian et al. [41] and Liew et al. [58], hence decreased the ionic conductivity. These peaks attributed to the recrystallization of $LiClO_4$ out of the film surface because the polymer host was unable to accommodate the salt. This leads to the recombination of ions thus decreased the conductivity [4]. The crystallinity peaks were found to be absent with the addition of plasticizer. This variation confirms a complete dissolution of the polymer electrolyte and the complexation between the polymer blend, $LiClO_4$ and glycerol [59]. The conductivity enhancement due to plasticization can also be explained by this XRD result. It can be seen that the XRD hump of the polymer blend containing 20 wt% glycerol is broader compared to the one containing 5 wt% glycerol, proving that the highest conducting electrolyte has the most amorphous structure. Dragunski and Pawlicka [60] reported that the crystalline peaks in the X-ray diffractogram of pure amylopectin-rich starch are absent in the diffractogram of starch-$LiClO_4$-glycerol complexes, confirming the amorphous structure of the electrolytes.

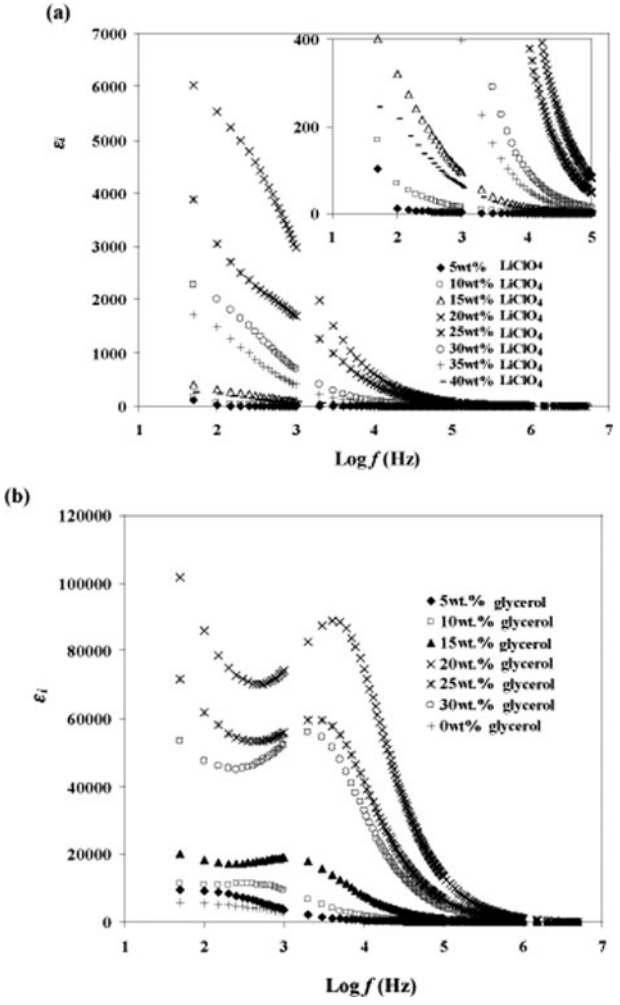

Figure 9. Plots of ε_i versus frequency for (a) salted and (b) plasticized systems. The inset figure in (a) shows an enlarge plot at low frequency.

Dielectric study

The dielectric study helps to understand the trend of conductivity and also gives the important insights of the polarization effect at the electrode/ electrolyte interfaces [61]. The equations for the dielectric constant, ε_r and dielectric loss, ε_i are as follow:

$$\varepsilon_r = \frac{Z_i}{\omega C_o (Z_r^2 + Z_i^2)} \tag{4}$$

$$\varepsilon_i = \frac{Z_r}{\omega C_o (Z_r^2 + Z_i^2)} \tag{5}$$

where Z_i is imaginary part of impedance, Z_r is real part of impedance, C_0 is vacuum capacitance and ω is angular frequency. Here, $C_0 = \varepsilon_0 A/t$ and $\omega = 2\pi f$, ε_0 is the permittivity of free space and f is the frequency. ε_r represents the material's stored charge, while ε_i represents the amount of energy loss to move ions and align dipoles when the electric field polarity reverses rapidly [62]. Figure 8 (a) and (b) show that the ε_r values of MC-starch-20 wt% $LiClO_4$ are the

highest in the salted system while the ε_r values of MC-starch-$LiClO_4$-20 wt% glycerol are the highest in plasticized system. An increase in dielectric constant is due to the increasing number of charge carriers in the space charge accumulation region [63]. The addition of glycerol which has high dielectric constant leads to a higher dissociation rate of the ions hence leads to conductivity enhancement [59]. Shukur et al. [64] reported that the dielectric constant result for starch-lithium iodide (LiI) and starch-LiI-glycerol electrolytes is in agreement with the conductivity result. When the polarity of ac stimulus reverses, ion translational diffusion and dipole orientation decelerate, stop, and accelerate in the reverse direction. This polarization process produces heat through internal friction which occurred when the ions overcome the opposition they encounter hence causes energy loss, ε_i [65]. At low-frequency region, the ions tend to diffuse and migrate along the field appropriately under the influence of an electric field. Since the ions are not transparent to the stainless steel electrodes, they accumulate and localized in a heterocharge layer at the electrode-electrolyte interface [65, 66]. Assuming that the thickness of the electrolyte is greater than the heterocharge layer, the charge density increases rapidly leading to electrode polarization [67]. This phenomenon has occurred in this work, as can be seen in Fig. 9 (a) and (b). The decrease in ε_r and ε_i at higher frequencies is ascribed to the decrease in charge accumulation [29]. As the frequency increased, the dipoles are unable to follow the direction of the field hence the orientation polarization stops.

Conclusion

MC-starch-$LiClO_4$ and MC-starch-$LiClO_4$-glycerol systems were successfully prepared via the solution casting technique. XRD and TGA results prove that 60 wt% MC-40 wt% starch was the most suitable ratio to serve as the polymer blend host due to its amorphous nature and thermally stable characteristics. FTIR analysis showed that the interaction occurred between the polymer host, salt and the plasticizer. In the salted system, the highest room temperature conductivity was obtained at $(3.26 \pm 1.12) \times 10^{-6}$ S cm^{-1} with the addition of 20 wt% $LiClO_4$. In the plasticized system, the highest room temperature conductivity was obtained at $(4.25 \pm 0.82) \times 10^{-4}$ S cm^{-1} on the addition of 20 wt% glycerol. The dielectric study has strengthened the conductivity trend. The plot of conductivity-temperature proves that all electrolytes obeyed the Arrhenius rule.

Acknowledgment

The authors would like to thank the University of Malaya for the financial support provided (Grant No. RP010A-13AFR).

References

[1] Taib, N. U., & Idris, N. H. (2014). *J. Membr. Sci.*, *468*, 149.
[2] Liew, C. W., Ramesh, S., & Arof, A.K. (2013). *Int. J. Hydrogen. Energ.*, *39*, 2917.
[3] Shukur, M. F., Ithnin, R., Illias, H. A., & Kadir, M. F. Z. (2013). *Opt. Mater.*, *35*, 1834.
[4] Kadir, M. F. Z., Majid, S. R., Arof, A. K. (2010). *Electrochim. Acta*, *55*, 1475.
[5] Riess, I. (2000). *Solid State Ionics*, *136–137*, 1119.
[6] Yusof, Y. M., Shukur, M. F., Illias, H. A., & Kadir, M. F. Z. (2014). *Phys. Scr.*, *89*, 035701.
[7] Yusof, Y. M., Majid, N. A, Kasmani, R. M., Illias, H. A., & Kadir, M. F. Z. (2014). *Mol. Cryst. Liq. Cryst.*, *603*, 73.
[8] Shukur, M. F., Yusof, Y. M., Zawawi, S. M. M., Illias, H. A., & Kadir, M. F. Z. (2013). *Phys. Scr.*, *T157*, 014050.

[9] Kadir, M. F. Z. A., Teo, L. P., Majid, S. R., & Arof, A. K. (2009). *Mater. Res. Innov*., *13*, 191.
[10] Yusof, Y. M., Illias, H. A., & Kadir, M. F. Z. (2014). *Ionics*, *20*, 1235.
[11] Shuhaimi, N. E. A., Teo, L. P., Woo, H. J., Majid, S. R., & Arof, A. K. (2012). *Polym. Bull*., *69*, 807.
[12] Pratap, R., & Chandra, S. (2013). *Polym. Bull*., *70*, 3075.
[13] Yap, Y. L., You, A. H., Teo, L. L., & Hanapei, H. (2013). *Int. J. Electrochem. Sci*., *8*, 2154.
[14] Wieczorek, W., & Stevens, J.R. (1997). *J. Phys. Chem. B*, *101*, 1529.
[15] Aziz, N. A. N., Idris, N. K., & Isa, M. I. N. (2010). *Int. J. Phys. Sci*., *5*, 748.
[16] Rajendran, S., Mahendran, O., & Krishnaveni, K. (2003). *J. New. Mat. Electr. Sys*., *6*, 25.
[17] Garcia, M. A., Pinotti, A., Martino, M. N., & Zaritzky, N. E. (2004). *Carbohyd. Polym*., *56*, 339.
[18] Park, H., Weller, C., Vergano, P., & Testin, R. (1993). *J. Food Sci*., *58*, 1361.
[19] Scoennberg, C., Nest, J. F., & Gandini, A. (1995). *Electrochim. Acta*, *40*, 2281.
[20] Morales, P. V., Nest, J. F., & Gandini, A. (1998). *Electrochim. Acta*, *43*, 1275.
[21] Tambelli, C. E., Donoso, J. P., Regiani, A. M., Pawlicka, A., Gandini, A., & LeNest, J. F. (2001). *Electrochim. Acta*, *46*, 1665.
[22] Jie, R., Hongye, F., Tianbin, R., & Weizhong, Y. (2009). *Carbohyd. Polym*., *77*, 576.
[23] Khiar, A. S. A., & Arof, A. K. (2010). *Ionics*, *16*, 123.
[24] Khiar, A. S. A., & Arof, A. K. (2011). *WASET*, *59*, 23.
[25] Xu, W., Belieres, J.-P., & Angell, C.A. (2001). *Chem. Mater*., *13*, 575.
[26] Shukur, M. F., Ithnin, R., & Kadir, M. F. Z. (2014). *Electrochim. Act*., *136*, 204.
[27] Ramya, C. S., Selvasekarapandian, S., Savitha, T., Hirankumar, G., Baskaran, R., Bhuvaneswari, M. S., & Angelo, P. C. (2006). *Eur. Polym. J*., *42*, 2672.
[28] Teoh, K. H., Ramesh, S., & Arof, A. K. (2012). *J. Solid State Electrochem*., *16*, 3165.
[29] El-Kader, M. F. H. A., & Ragab, H. S. (2013). *Ionics*, *19*, 361.
[30] Kato, T., Yokoyama, M., & Takahashi, A. (1978). *Colloid & Polymer Sci*., *256*, 15.
[31] Fadzallah, I.A., Majid, S.R., Careem, M.A., & Arof, A.K. (2014). *J. Membrane Sci*., *463*, 65.
[32] Samsudin, A. S., Lai, H. M, & Isa, M. I. N. (2014). *Electrochim. Acta*, *129*, 1.
[33] Huang, F-. Y. (2012). *Polymers*, *4*, 1012.
[34] Ran, Y., Yin, Z., Ding, Z., Guo, H., & Yang, J. (2013). *Ionics*, *19*, 757.
[35] Ramesh, S., Shanti, R., & Morris, E. (2012). *Solid State Sciences*, *14*, 182.
[36] Mano, J. F., Koniarova, D., & Reis, R. L. (2003). *J. Mater. Sci.-Mater. M*., *14*, 127.
[37] Jagadish, R. S., & Raj, Baldev (2011). *Food Hydrocolloid*., *25*, 1572.
[38] Guru, G. S., Prasad, P., Shivakumar, H. R., & Rai, S. K. (2012). *IJRPC*, 957.
[39] Jingjid, S., Damrongsakkul, S., & Rimdusit, S. (2006). *The Fourth Thailand Materials Science and Technology Conference*, Thailand.
[40] Nik Aziz, N. A., Idris, N. K., & Isa, M. I. N. (2010). *Int. J. Polymer Anal. Char*., *15*, 319.
[41] Kulasekarapandian, K., Jayanthi, S., Muthukumari, A., Arulsankar, A., & Sundaresan, B. (2013). *IJERD*, 5, 30.
[42] Kumar, M., Tiwari, T., & Srivastava, N. (2012). *Carbohydr. Polym*., *88*, 54.
[43] Sudhakar, Y. N., Selvakumar, M., & Krishna Bhat, D. (2013). *Ionics*, *19*, 277.
[44] Arof, A. K., Shuhaimi, N. E. A., Alias, N. A., Kufian, M. Z., & Majid, S. R. (2010). *J. Solid State Electrochem*., *14*, 2145.
[45] Buraidah, M. H., Teo, L. P., Majid, S. R., & Arof, A. K. (2009). *Physica B*, *404*, 1373.
[46] Ramesh, S., & Arof, A. K. (2001). *Mater. Sci. Eng. B*, *85*, 11.
[47] Johan, M. R., & Ting, L. M. (2011). *Int. J. Electrochem. Sci*., *6*, 4737.
[48] Bergo, P. V. A., Sobral, P. J. A., & Prison, J. M. (2009). *Gene Conserve*, *32*, 727.
[49] Ibrahim, S., & Johan, M. R. (2012). *Int. J. Electrochem. Sci*., 7, 2596.
[50] Pawlicka, A., Sabadini, A. C., Raphael, E., & Dragunski, D. C. (2008). *Mol. Cryst. Liq. Cryst*., 485, 804.
[51] Buraidah, M. H., & Arof, A. K. (2011). *J. Non-Cryst. Solids*, *357*, 3261.
[52] Winie, T., Ramesh, S., & Arof, A. K. (2009). *Physica B*, *404*, 4308.
[53] Rajendran, S., Sivakumar, M., & Subadevi, R. (2004). *Mater. Lett*., *58*, 641.
[54] Harun, N. I., Ali, R. M., Ali, A. M. M., & Yahya, M. Z. A. (2011). *Mater. Res. Innov*., *15*, S168.
[55] Anderson, O. L., & Stuart, D. A. (1954). *J. Am. Ceram. Soc*., *37*, 573.
[56] Hodge, R. M., Edward, G. H., & Simon, G. P. (1996). *Polymer*, *37*, 1371.
[57] Khiar, A. S. A., & Arof, A. K. (2010). *Ionic*, *16*, 123.

[58] Liew, C. W., Ong, Y. S., Lim, J. Y., Lim, C. S., Teoh, K. H., & Ramesh, S. (2013). *Int. J. Electrochem. Sci*., *8*, 7779.
[59] Chew, K. W., Ng, T. C., & How, Z. H. (2013). *Int. J. Electrochem. Sci*., *8*, 6354.
[60] Dragunski, D. C., & Pawlicka, A. (2002). *Mol. Cryst. Liq. Cryst*., *374*, 561.
[61] Wintersgill, M. C., Fontanella, J. J., Pak, Y. S., Greenbaum, S. G., Al-Mudaris, A., Chadwick, A. V. (1989). *Polymer*, *30*, 1123.
[62] Woo, H. J., Majid, S. R., & Arof, A. K. (2012). *Mater. Chem. Phy*., *134*, 755.
[63] Sudhakar, Y. N., & Selvakumar, M. (2013). *J. Appl. Electrochem*., *43*, 21.
[64] Shukur, M. F., Ibrahim, F. M., Majid, N. A., Ithnin, R., & Kadir, M. F. Z. (2013). *Phys. Scr*., *88*, 025601.
[65] Woo, H. J., Majid, S. R., & Arof, A. K. (2012). *Mater. Chem. Phys*., *134*, 755.
[66] Kufian, M. Z., Aziz, M. F., Shukur, M. F., Rahim, A. S., Ariffin, N. E., Shuhaimi, N. E. A., Majid, S. R., Yahya, R., & Arof, A. K. (2012). *Solid State Ion*, *208*, 36.
[67] Howell, F. S., Bose, R. A., Macedo, P. B., & Moynihan, C. T. (1974). *J. Phys. Chem*., *78*, 639.